



SYNTHESIS, MAGNETIC, SPECTRAL, THERMAL AND ANTIMICROBIAL STUDIES OF MN(II), FE(III), CO(II), NI(II) AND CU(II) COMPLEXES OF CHALCONES DERIVED FROM DEHYDROACETIC ACID

Vaibhav N. Patange

Department of Chemistry, Shri Chhatrapati Shivaji College, Omerga,
Dist-Osmanabad-, Maharashtra, India.

ABSTRACT

Transition metal complexes of chalcones derived from condensation of 3-acetyl-6-methyl pyran-2,4(3H)-dione (dehydroacetic acid) and Benzaldehyde (HL^1) or *m*-nitrobenzaldehyde (HL^2) are reported and characterized based on elemental analysis, conductometry, thermal analysis, magnetic, IR, 1H NMR, UV-VIS, X-ray diffraction and antimicrobial study. From the analytical and thermal data, the stoichiometry of the complexes has been found to be 1:2 (metal : ligand). Distorted octahedral geometry for Cu(II) complex and octahedral geometries for Mn(II), Fe(III), Co(II) and Ni(II) complexes are proposed. The molar conductance data reveals that all the metal chelates were non-electrolytes. The complexes of ligand HL^2 were chosen for thermal study. Kinetic parameters, (n , E^* , A , ΔS^* and ΔG^*) are calculated from TG and DTA curves using Coats-Redfern method. The thermal stability of the complexes were studied using thermogravimetry and the decomposition schemes of the complexes were given. The powder X-ray diffraction suggests monoclinic crystal system for all the complexes of ligand HL^2 . The ligands and their metal complexes were screened for antibacterial activity against gram positive bacteria (*Staphylococcus aureus*) and gram negative bacteria (*Escherichia coli*), and the fungicidal activity against *Aspergillus flavus*, *Curvularia lunata* and *Penicillium notatum*.

KEYWORDS: Dehydroacetic acid, Chalcones, Thermal study, Kinetic parameters, powder X-ray diffraction, Antimicrobial study.

1. INTRODUCTION

Dehydroacetic acid (3-acetyl-6-methyl-2H-pyran-2,4(3H)-dione), a biologically active compound has shown to have good antibiotic and antifungal effects, besides showing strong antiseptic properties [1]. Chalcones are associated with many biological activities due to the presence of α , β unsaturated system as evidenced from their antimicrobial, molluscicidal, anti-inflammatory, antiprotozoal, anti-oxidant, analgesic and anti-trichomonal [2-8] activities. A number of β -dicarbonyl compounds in which the carbonyl function(s) bonded to C=C linkage(s) have gained considerable importance [9] mainly because of the fact that such compounds are structurally related to the active chemical constituents of several traditional medicinal plants and their metal complexes possess interesting biochemical properties [9-13]. Therefore, synthesis and characterization of such unsaturated carbonyl system and their metal complexes have tremendous importance [14-16]. Thus, the main target of the present study is to synthesize some transition metal complexes of dehydroacetic acid chalcone in which the carbonyl group is directly linked to α , β unsaturated system and investigate their bonding, thermal, spectral and microbial characteristics (Figure 1).

2. EXPERIMENTAL

2.1. Materials and instrumentation

Dehydroacetic acid was purchased from Merck and was used as supplied. Benzaldehyde and m-nitrobenzaldehyde used for the preparation of ligand were from Aldrich. Metal chlorides used for the complex preparation were from BDH. A.R.grade solvents were used for spectral measurements. The carbon, hydrogen and nitrogen content in each sample were determined on Perkin Elmer (2400) CHNS analyzer. IR spectra (nujol) in the range of 4000-450 cm^{-1} were recorded on Perkin Elmer (C-75430) spectrometer. ^1H NMR spectra were carried out in CDCl_3 at room temperature using TMS as internal standard on a Varian Mercury YH 300 MHz. The metal contents were determined by AAS on Perkin Elmer PE-Analyst 300. The TG-DTA measurements were carried out on a PerkinElmer TA/SDT-2960 in dry nitrogen atmosphere and a heating rate of $10^\circ\text{C}/\text{min}$. The powder XRD were recorded on Philips 3701. Electronic spectra were recorded in DMF solution on Shimadzu UV-1601 spectrophotometer. Magnetic susceptibility measurements of the complexes were carried out using a Gouy balance at room temperature using $\text{Hg}[\text{Co}(\text{SCN})_4]$ as calibrant. Molar conductivity was measured on an Elico CM180 conductivity meter with a dip-type cell using 10^{-3} M solution of complexes in DMF.

2.2. Synthesis of ligand

A solution of 0.01 mole of dehydroacetic acid, 10 drops of piperidine and 0.01 mole of aldehyde (benzaldehyde or m-nitrobenzaldehyde) in 25 ml chloroform was refluxed for 8-10 hours. 10 ml of the chloroform-water azeotrope mixture was separated by distillation. Crystals of product were separated on slow evaporation of the remaining chloroform and recrystallised from ethyl acetate.

2.3 Synthesis of metal complexes

To a chloroform solution (30 ml) of the ligand (10 mmol), methanolic solution (20 ml) of metal chloride (5 mmol) was added with constant stirring. The pH of the reaction mixture was maintained around 7.5-8.0 by adding 10% methanolic solution of ammonia. It was then refluxed for 2 hours. The resulting metal complex was filtered hot and washed with chloroform, methanol and petroleum-ether and dried over calcium chloride in vacuum desiccator.

3. RESULTS AND DISCUSSION

The elemental analysis show 1:2 (metal : ligand) stoichiometry for all the complexes (Figure 2). The analytical data of the ligand and the complexes are given in Table 1. It corresponds well with the general formula $[\text{M}(\text{L}^{1\text{or}2})_2(\text{H}_2\text{O})_2]$, where $\text{M} = \text{Mn}(\text{II}), \text{Co}(\text{II}), \text{Cu}(\text{II}), [\text{M}(\text{L}^{1\text{or}2})_2(\text{Cl})(\text{H}_2\text{O})]$, where $\text{M} = \text{Fe}(\text{III})$ and $\text{L}^1 = \text{C}_{15}\text{H}_{11}\text{O}_4$, $\text{L}^2 = \text{C}_{15}\text{H}_{10}\text{NO}_6$. The presence of water of crystallization is confirmed by TGA-DTA analysis. The presence of chlorine in Fe(III) complexes was evident from Volhard's test. The low conductance of the chelate solution supports the non-electrolytic nature of the metal complexes.

3.1. ^1H -NMR spectrum

ligand HL^1 ;

The ^1H -NMR (300 MHz, CDCl_3 , δ , ppm): 2.27(S, 3H, $\text{C}_6\text{-CH}_3$), 6.03(S, 1H, $\text{C}_5\text{-H}$), 7.2-8.32(m, 7H, phenyl ring and -CH=CH-), 16.3(S, 1H, $\text{C}_4\text{-OH}$).

ligand HL^2 ;

The ^1H -NMR (300 MHz, CDCl_3 , δ , ppm): 2.35(S, 3H, $\text{C}_6\text{-CH}_3$), 6.03(S, 1H, $\text{C}_5\text{-H}$), 7.9-8.48(m, 6H, phenyl ring and -CH=CH-), 16.5(S, 1H, $\text{C}_4\text{-OH}$).

3.2. IR Spectra

The IR spectrum of the ligands shows bands at 3162-3120, 1720-1713, 1760-1659 and 1253-1222 cm^{-1} assignable to νOH (phenolic hydrogen bonded), $\nu\text{C=O}$ (lactone carbonyl), $\nu\text{C=O}$ (acetyl carbonyl) and

ν C-O (phenolic) stretching mode respectively [17-18] (Table 2). In the IR spectra of all the metal chelates, no band is observed in the region 3162-3120 cm^{-1} . Instead, in its place broad band characteristic of ν OH of coordination water is observed in the region 3500-3200 cm^{-1} . The presence of coordinated water is further confirmed by the appearance of non-ligand band in the region 830-840 cm^{-1} , assignable to the rocking mode of water [19]. Besides, it is also established and supported by TG and DTA analysis. The absence of ν OH (phenolic) at 3162-3120 cm^{-1} suggests subsequent deprotonation of the phenolic group and coordination of phenolic oxygen to the metal ion. This is supported by an upward shift in ν C-O (phenolic) to the extent 20 – 40 cm^{-1} [20]. The ν C=O (acetyl carbonyl) is shifted to the lower energy with respect to the free ligand, suggesting the participation of ν C=O (acetyl carbonyl) in coordination [17-18, 20]. IR spectra of all the compounds showed a prominent band at $\sim 1377 \text{ cm}^{-1}$ and $\sim 970 \text{ cm}^{-1}$ typical to ν C-O-C and trans –CH=CH- absorption. The presence of new bands in the region 600 - 450 cm^{-1} can be assigned to ν M-O vibrations [19].

The pH-metric measurements for $3 \times 10^{-3} \text{ M}$ of 75% (v/v) methanol-water solution of the ligand indicated that only one proton dissociates together with the value of pK_a (9.95) for HL^1 and pK_a (9.87) for HL^2 suggesting that the ligands behave as a weak monoprotic acid. The value of pK_a reveals that the proton dissociated from the phenolic OH group.

Hence, the ligands coordinated with the metal ions as monoprotic bidentate and coordination takes place via the acetyl and phenolic oxygen of dehydroacetic acid moiety as shown in Fig. 1.

3.3. Magnetic and Electronic absorption spectra

The magnetic and electronic spectral data is shown in Table 2. The data is in relevance to the proposed structure of the complexes (Fig 1). The Cu(II) complexes in DMF reveal one broad band at 15 128, 25 380 cm^{-1} for ligand HL^1 and 14 925, 25 316 cm^{-1} , for ligand HL^2 , assignable to ${}^2\text{E}_g \rightarrow {}^2\text{T}_{2g}$ transition and due to charge transfer respectively. The observed magnetic moment value for the Cu(II) complexes is in the range 1.88-1.98 BM. The electronic spectral data [21] coupled with magnetic moment value suggest a distorted octahedral geometry for the Cu (II) complexes [22]. The electronic spectrum of Ni(II) complexes displays three bands at 9870, 15 384 and 24 937 cm^{-1} for HL^1 , 9900, 15 360 and 24 875 cm^{-1} for HL^2 , assignable to ${}^3\text{A}_{2g} \rightarrow {}^3\text{T}_{2g}$ (F) (ν_1), ${}^3\text{A}_{2g} \rightarrow {}^3\text{T}_{1g}$ (F) (ν_2) and ${}^3\text{A}_{2g} \rightarrow {}^3\text{T}_{1g}$ (P) (ν_3) transitions respectively. This in accordance with earlier reported values for the octahedral Ni(II) complexes [23,24]. The reduction of Racah parameters (B) and Nephelauxetic effect (β) from the free ion value suggest appreciable amount of covalent character in the metal ligand bonds [24]. The calculated values of 10Dq , B, ν_2/ν_1 and β (Table 2) lie in the range reported for octahedral geometry. The normal magnetic moment 2.95 – 3.02 B.M confirms the proposed geometry. The Co(II) complexes shows three transitions at 9794, 18 622 and 23 753 cm^{-1} for HL^1 , 9900, 19 193 and 23 640 cm^{-1} for HL^2 , assignable to ${}^4\text{T}_{1g}(\text{F}) \rightarrow {}^4\text{T}_{2g}(\text{F})$ (ν_1), ${}^4\text{T}_{1g}(\text{F}) \rightarrow {}^4\text{A}_{2g}(\text{F})$ (ν_2) and ${}^4\text{T}_{1g}(\text{F}) \rightarrow {}^4\text{T}_{1g}(\text{P})$ (ν_3) transitions respectively [24,25]. The calculated values of 10Dq , B, ν_2/ν_1 and β together with magnetic moment value of Co(II) complexes (Table 2) suggest octahedral geometry.

The obtained values of LFSE (10Dq) determine the stability of the complexes and follows the order in terms of metal ion $\text{Cu(II)} > \text{Ni(II)} > \text{Co(II)}$ for ligand HL^1 and HL^2 . The Fe(III) complexes of ligand HL^1 and HL^2 shows three bands at 14 706, 21 008, 24 876 cm^{-1} and 14 641, 21 052, 24 605 cm^{-1} , assignable to ${}^6\text{A}_{1g} \rightarrow {}^4\text{T}_{1g}(\text{G})$, ${}^6\text{A}_{1g} \rightarrow {}^4\text{T}_{2g}(\text{G})$ and ${}^6\text{A}_{1g} \rightarrow {}^4\text{E}_g(\text{G})$ transitions respectively. The electronic spectral data together with reported magnetic moment value of Fe(III) complexes (Table 2) suggest high spin octahedral geometry [24,26]. The electronic spectrum of Mn(II) complex of HL^1 and HL^2 displays three bands at 17 513, 19 685, 33 557 cm^{-1} and 18 382, 19 083, 33 444 cm^{-1} . The first two bands of Mn(II) complexes corresponds to ${}^6\text{A}_{1g} \rightarrow {}^4\text{T}_{1g}(\text{G})$, ${}^6\text{A}_{1g} \rightarrow {}^4\text{T}_{2g}(\text{G})$ transitions and third band may be due to charge transfer respectively. The electronic spectral data together with reported magnetic moment value of Mn(II) complexes (Table 2) suggest high spin octahedral geometry. [24].

3.4. Thermal Analysis

The Mn(II), Fe(III), Co(II), Ni(II) and Cu(II) complexes of ligand HL² was chosen for thermal study. The TG curve of the complexes of ligand HL² shows three steps of decomposition except Co(II) complex wherein four steps are observed.

In the TG curve of Mn(II) complex, the first step shows a steep slope between 185-225°C with a mass loss of 5.0%(calcd., 5.21%), indicates the removal of two molecules of coordinated water, an endothermic peak in the range 190-220°C(ΔT_{min}=213°C) in DTA corresponds to dehydration step. The anhydrous compound in second step decomposes within a short temperature range from 320-450°C with a 38.5 % mass loss (calcd, 39.04%), an exotherm between 340 and 420°C with ΔT_{max} = 366°C in DTA. This step may be attributed to the removal of non-coordinated part of the ligand i.e., phenyl ring including β carbon [C₁₄H₁₀N₂O₄]. The third step corresponds to decomposition of coordinated part of the ligand and in the range of 500-890°C with a mass loss 46.5 % (calcd., 45.49%). A broad endotherm is observed for this step. The mass of the final residue corresponds to stable MnO, 10.0 % (calcd., 10.26%) (Scheme 1). In thermal study of Fe(III) complex, an inclined slope from 175°-220°C in TG curve with mass loss 8.0% (calcd., 7.53%) indicates the removal of one molecule of water and one chloride ion, an endothermic peak in the range 180-240°C is observed in DTA (ΔT_{min} = 207°C). The complex continues to second step decomposition in between temperature 260 and 400°C with 37.5 % mass loss (calcd. 38.04 %). An exothermic peak between 250-380°C (ΔT_{max} = 345°C) in DTA, attributed to the removal of non-coordinating part of the ligand. The third step corresponds to slow decomposition of remaining part of the ligand upto 850 °C with a mass loss 43.5 % (calcd. 44.31 %). The mass of the final residue 11.0 % (calcd. 10.12%) corresponds to FeO (Scheme 2). The thermal decomposition profile of Co(II) complex show no weight loss up to 140°C. Slow mass loss of 5.0 % (calcd. 5.18 %) is observed in the range 140-200°C. Two endothermic peaks between 150-165°C (ΔT_{min} = 159°C) and 185-200°C(ΔT_{min} = 197°C), correspond to loss of two molecules of water. The third step of decomposition is very rapid and in between temperature 360 and 380°C with 39.0% mass loss (calcd. 38.82%). A broad exothermic peak between 270-375°C (ΔT_{max} = 371°C) in DTA, attributed to the removal of non-coordinating part of the ligand. The mass loss continues and follows slow decomposition of remaining part of the ligand 45.0 % (calcd., 45.22 %). The mass of the final residue corresponds to CoO, 11.0% (calcd. 10.78 %) (Scheme 1). The thermal decomposition profile of Ni(II) complex show weight loss 5.0 % (calcd., 5.18 %) in the range 160-175°C indicates the removal of two coordinated water molecule. An endothermic peak in DTA between 160-185°C (ΔT_{min} = 172°C), correspond to dehydration. The second step of decomposition is in between 260 and 425°C with 38.0 % mass loss (calcd., 38.83 %). A broad exothermic peak between 280-450°C (ΔT_{max} = 360.0°C) in DTA, attributed to the removal of non-coordinating part of the ligand. The mass loss continues and follows slow decomposition of remaining part of the ligand upto 900°C with 46.0 % (calcd. 45.25 %). A broad endothermic peak between 550-850°C is observed in DTA. The mass of the final residue 11.0 % (calcd. 10.74 %), corresponds to NiO (Scheme 1). In the TG curve of Cu(II) complex, the mass loss starts from 130°C and an inclined slope from 160-185°C with a mass loss of 5.5% (calcd., 5.14 %), indicates the removal of two molecules of coordinated water, an endothermic peak in the range 170-185°C (ΔT_{min}=168°C) in DTA corresponds to dehydration step. The second step decomposition continues in TG curve from 295°C upto 475°C, with a mass loss 39.5 % (calcd., 38.57 %), an exothermic peak ΔT_{max} = 382°C in DTA may be attributed to the removal of non-coordinated part of the ligand. The third step corresponds to decomposition of coordinated part of the ligand and in the range of 520-950°C with a mass loss 44.0 % (calcd., 44.93 %). A broad endotherm is observed for this step. The mass of the final residue corresponds to stable CuO, 11.0 % (calcd., 11.36 %) (Scheme 1). The kinetic parameters i.e., n (order of reaction), E* (energy of activation), Z (pre-exponential factor), ΔS* (entropy) and ΔG* (free energy change) for all the decomposition step were calculated from non-isothermal TG curves using Coats-Redfern method [27, 28].

$$\log \left[\frac{1 - (1 - \alpha)^{1-n}}{(1-n)T^2} \right] = \log \frac{ZR}{Eq} \left[1 - \frac{2RT}{E} \right] - \frac{E}{2.303R} \cdot \frac{1}{T}$$

Where the terms have their usual meaning. The left-hand side of equation was plotted against $1/T$. By using different value of order of reaction, straight line was fitted by regression. The highest value of correlation coefficient gave the correct value of 'n'. From the slope and intercept, E and Z values were calculated. Using E* and Z values, the values of ΔS^* and ΔG^* were determined [28].

3.5 Powder X-Ray diffraction

The oxide residue of Mn(II), Fe(III), Co(II), Ni(II) and Cu(II) complexes of ligand HL² obtained at 1000°C by thermal analysis were grounded and subjected to XRD analysis. The XRD powder diffractogram of metal oxide residue of Mn(II), Fe(III), Co(II), Ni(II) and Cu(II) complexes of ligand HL² are shown in Figure 3. It is clear from the Table 4 that the final decomposition product of complexes of HL² was there corresponding oxides whose XRD data matches the reference data. This confirms that the predicted decomposition steps of complexes are correct.

Since single crystal of the complexes could not be isolated from any common solvent therefore powder X-ray diffraction of complexes of ligand HL² were also carried out at room temperature. The diffractogram of [C₃₀H₂₄N₂O₁₄Cu] complex records thirteen reflections between 20 to 80°(2θ) with maxima at 2θ = 25.12° corresponding to d value 3.5480 Å. The diffractogram of [C₃₀H₂₄N₂O₁₄Ni] complex records twelve reflections between 05 to 80°(2θ) with maxima at 2θ = 6.65° corresponding to d value 13.2882 Å, where as [C₃₀H₂₄N₂O₁₄Co] complex records twelve reflections with maxima at 2θ = 26.48° corresponding to d value 3.3639 Å. The diffractogram of [C₃₀H₂₄N₂O₁₄Mn] complex records sixteen reflections between 05 to 80°(2θ) with maxima at 2θ = 23.69° corresponding to d value 3.753 Å. The diffractogram of [C₃₀H₂₂N₂O₁₃ClFe] complex records fourteen reflections between 05 to 80°(2θ) with maxima at 2θ = 7.08° corresponding to d value 12.4815 Å. The X-Ray diffraction pattern of Mn(II), Fe(III), Co(II), Ni(II) and Cu(II) complexes with respect to prominent peaks having relative intensity greater than 10% have been indexed by using computer software [29]. The above indexed method also yielded miller indices (hkl), unit cell parameters and volume of unit cell. The unit cell of the Mn(II) complex yielded values for lattice constant a = 9.2078 Å, b = 11.4978 Å, c = 9.1222 Å and unit cell volume V = 775.06 Å³. The unit cell of the Fe(III) complex yielded values for lattice constant a = 15.2026 Å, b = 8.4837 Å, c = 12.8016 Å and unit cell volume V = 1608.19 Å³. The unit cell of the Co(II) complex yielded values for lattice constant a = 17.3695 Å, b = 14.9963 Å, c = 4.6431 Å and unit cell volume V = 1207.51 Å³. The unit cell of the Ni(II) complex yielded values for lattice constant a = 10.7852 Å, b = 13.2731 Å, c = 8.9640 Å and unit cell volume V = 1153.94 Å³ and the unit cell of the Cu(II) complex yielded values for lattice constant a = 8.5969 Å, b = 14.4629 Å, c = 7.7356 Å and unit cell volume V = 961.72 Å³. In conjunction with these evaluated cell parameters, the condition such as a ≠ b ≠ c and α = δ = 90° ≠ β required for the samples to be monoclinic for Mn(II), Fe(III), Co(II), Ni(II) and Cu(II) were tested and found to be satisfactory.

The experimental density values of the complexes were determined by using specific gravity method [30]. By using this value of density, molecular weight of the complexes, Avogadro's number and volume of unit cell, the number of molecules (n) per unit cell were calculated by using equation $\rho = nm/NV$ and was found to be 1 for Fe(III), complex and 2 for Mn(II) Co(II), Ni(II) and Cu(II) complexes. With this value, theoretical densities have been computed. The experimental density values of Mn(II), Fe(III), Co(II), Ni(II) and Cu(II) complexes are 1.2541, 1.4503, 1.8978, 1.9756 and 2.5106 g cm⁻³ respectively. The theoretical density values of Mn(II), Fe(III), Co(II), Ni(II) and Cu(II) complexes are 1.2675, 1.4655, 1.9128, 2.0009 and 2.5362 g cm⁻³ respectively. When experimental density value of the complexes compared with the theoretical density value, it is found that there is good agreement within the limits of experimental errors. The particle size [31] of Mn(II), Fe(III), Co(II), Ni(II) and Cu(II) complexes were found to be 140.65, 94.20, 76.37, 146.53 and 266.1 Å respectively.

4. ANTIMICROBIAL SCREENING

The ligand and its metal complexes have been screened against antibacterial and antifungal activities in vitro.

4.1 Antibacterial activity

The ligand and their metal complexes were screened for antibacterial activity against gram positive bacteria, *Staphylococcus aureus* and gram negative bacteria, *Escherichia coli* by paper disc plate method [32]. The compounds were tested at the concentration of 500 and 1000 ppm in DMF and compared with known antibiotic viz Ciproflaxin at the same concentration. It was observed that ligand HL¹ and its complexes do not show any activity whereas, ligand HL² show weak antibacterial activity and their complexes show moderate activity against both the bacteria's.

4.2 Antifungal Activity

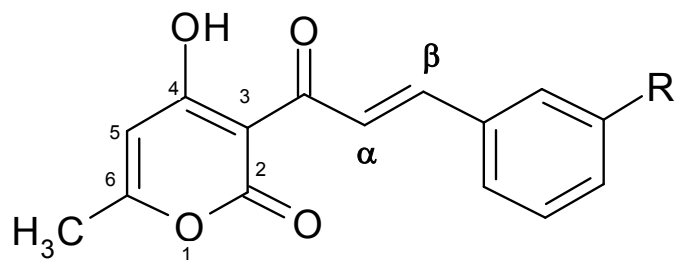
To evaluate fungicidal activity of the ligand and their corresponding metal complexes, their effect on the growth of *Aspergillus flavus*, *Curvularia lunata* and *Penicillium notatum* was studied. The ligand and their corresponding metal chelates in DMF were screened by mycelia dry weight method [33] in vitro for their fungicidal activity in glucose nitrate media. The compounds were tested at the concentration of 125 and 250 ppm in DMF and compared with known antifungal drug viz Griseofulvin. The ligand HL¹ exhibited 15-20 % inhibition at 125 ppm and 35-40% inhibition at 250 ppm concentration, whereas the ligand HL² exhibited 25-30 % inhibition at 125 ppm and 45-50% inhibition at 250 ppm concentration for all the three fungi. Due to synergistic combination of the coordinated metal ions with the ligand, the inhibition by metal complexes of HL¹ has been increased by 30 – 55% and 40 –70 % for 125 and 250 ppm concentration and the inhibition by metal complexes of HL² has been increased by 30 -80 % and 60 – 99 % respectively for all the three fungi. The order of inhibition with respect to metal ions is Cu>Ni>Co>Mn>Fe for HL¹ and for HL² it is Cu>Ni>Mn>Co>Fe. The antifungal data reveals that the metal complexes are superior to the free ligand and the inhibition decreased the concentration decreased .

CONCLUSION

The results of this investigation support the suggested structure i.e., distorted octahedral geometry for Cu(II) complexes and an octahedral geometry for Mn(II), Fe(III), Co(II) and Ni(II) complexes. The ligands behave as bidentate, coordinating through oxygen of phenolic and acetyl carbonyl group of dehydroacetic acid moiety. The thermal studies of the complexes indicate that the complexes are thermally stable. The complexes are biologically active and exhibit enhanced antifungal activities compared to their parent ligand.

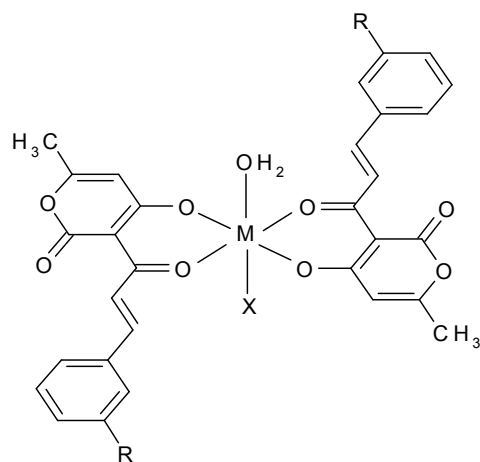
ACKNOWLEDGEMENTS

One of us (VNP) is grateful to the UGC (WRO) pune, for the award of Teacher fellowship under FIP in Xth plan. The authors are also thankful to Dr. T.K.Chondhekar, Dept of Chemistry Dr. B. A. M. University, Aurangabad, for valuable suggestions.



Where R = -H or -NO₂

Figure 1: Structure of Ligand



R = - H or - NO₂

X = H₂O; When M = Mn(II), Co(II), Ni(II), and Cu(II)

X = Cl; When M = Fe(III)

Figure 2: The proposed structure of the complexes

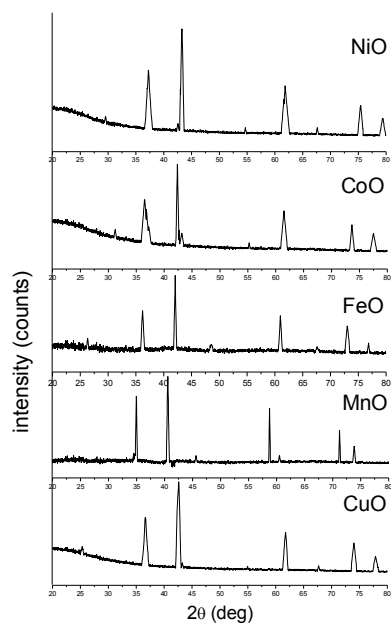
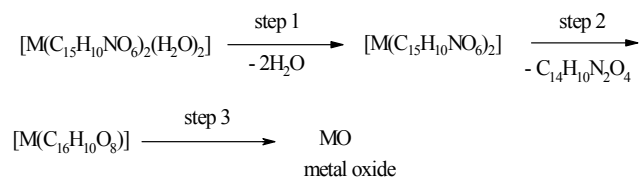
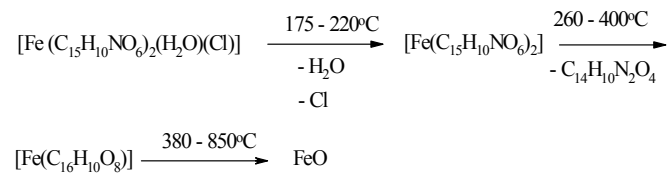


Figure 3. XRD powder diffractogram of the metal oxide residue.



Where M = Mn(II), Co(II), Ni(II), Cu(II)

Scheme 1



Scheme 2

Table 1: Physical characterization, analytical and molar conductance data of the Compounds

Compound	F.W	M.P °C	Yield %	Color	Found (Calc.)%					λ_m Mho cm^2 mol^{-1}
					C	H	N	Cl	M	
Ligand HL ¹ C ₁₅ H ₁₂ O ₄	256.3	131	59	yellow	70.21 (70.31)	4.63 (4.72)	-	-	-	-
[C ₃₀ H ₂₆ O ₁₀ Mn]	601.5	192	64	Brown	60.21 (59.95)	4.43 (4.36)	-	-	8.93 (9.13)	13.1
[C ₃₀ H ₂₄ O ₉ ClFe]	619.8	195	68	Red	58.01 (58.13)	4.02 (3.90)	-	5.63 (5.72)	9.12 (9.00)	12.2
[C ₃₀ H ₂₆ O ₁₀ Co]	605.5	265	69	Light Brown	60.12 (59.51)	4.21 (4.33)	-	-	9.53 (9.73)	17.7
[C ₃₀ H ₂₆ O ₁₀ Ni]	605.2	249	65	Pale green	60.15 (59.53)	4.29 (4.34)	-	-	9.50 (9.69)	12.1
[C ₃₀ H ₂₆ O ₁₀ Cu]	610.1	273	73	Green	59.12 (59.06)	4.32 (4.30)	-	-	10.23 (10.41)	17.5
Ligand HL ² C ₁₅ H ₁₁ NO ₆	301.3	191	54	Yellow	59.52 (59.80)	3.51 (3.68)	4.57 (4.65)	-	-	-
[C ₃₀ H ₂₄ N ₂ O ₁₄ Mn]	691.5	>300	64	Brown	51.94 (52.10)	3.41 (3.49)	3.99 (4.05)	-	7.81 (7.94)	3.1
[C ₃₀ H ₂₂ N ₂ O ₁₃ ClFe]	709.7	>300	63	Red	51.02 (50.77)	3.02 (3.12)	3.89 (3.95)	4.93 (5.00)	7.71 (7.87)	2.2
[C ₃₀ H ₂₄ N ₂ O ₁₄ Co]	695.5	>300	61	Light Brown	52.21 (51.81)	3.51 (3.48)	4.12 (4.03)	-	8.22 (8.47)	7.7
[C ₃₀ H ₂₄ N ₂ O ₁₄ Ni]	695.2	>300	67	Pale green	51.99 (51.82)	3.51 (3.48)	4.18 (4.03)	-	8.36 (8.44)	2.1
[C ₃₀ H ₂₄ N ₂ O ₁₄ Cu]	700.1	>300	63	Green	52.08 (51.46)	3.55 (3.45)	4.21 (4.00)	-	8.93 (9.07)	5.1

Table 2: Characteristic IR frequencies (cm⁻¹), magnetic and ligand field parameters.

Complex	ν_{OH}	$\nu_{\text{C=O}}$ (lactone carbonyl)	$\nu_{\text{C=O}}$ (acetyl carbonyl)	$\nu_{\text{C-O}}$ (phenolic)	ν_{NO_2}	$\nu_{\text{M-O}}$	μ_{eff} BM	10 Dq cm^{-1}	B cm^{-1}	β	ν_2/ν_1	LFSE Kcal mole^{-1}
HL ¹ C ₁₆ H ₁₄ O ₅	3162(b)	1712(m)	1659(m)	1253(m)	-	-	-	-	-	-	-	-
HL ² C ₁₅ H ₁₁ NO ₆	3120(b)	1722(s)	1660(m)	1222(m)	1571(s)	-	-	-	-	-	-	-
[Mn(L ¹) ₂ (H ₂ O) ₂]	3374(b)	1710(m)	1625(m)	1281(m)	-	526(m) 568(m)	5.84	-	-	-	-	-
[Mn(L ²) ₂ (H ₂ O) ₂]	3371(b)	1715(s)	1643(s)	1250(m)	1574(s)	473(m) 585(m) 533(m)	5.98	-	-	-	-	-
[Fe(L ¹) ₂ (Cl)(H ₂ O)]	3374(b)	1719(s)	1622(s)	1273(m)	-	493(m) 533(m) 582(m)	6.0	-	-	-	-	-
[Fe(L ²) ₂ (Cl)(H ₂ O)]	3372(b)	1716(m)	1642(m)	1245(m)	1573(m)	534(m) 585(w)	5.99	-	-	-	-	-

[Co(L ¹) ₂ (H ₂ O) ₂]	3357(b)	1708(s)	1626(s)	1263(m)	-	530(m) 578(m)	4.53	9794	866.8	0.89	1.90	25.22
[Co(L ²) ₂ (H ₂ O) ₂]	3355(b)	1715(s)	1635(m)	1251(m)	1568(s)	458(m) 555(m) 532(w)	5.10	9293	875.5	0.90	1.93	26.55
[Ni(L ¹) ₂ (H ₂ O) ₂]	3348(b)	1709(m)	1626(m)	1280(m)	-	485(m) 498(m) 531(m)	2.95	9708	746.5	0.71	1.58	27.73
[Ni(L ²) ₂ (H ₂ O) ₂]	3356(b)	1712(m)	1636(m)	1234(m)	1566(s)	480(w) 595(m)	3.02	9900	702.3	0.64	1.55	28.28
[Cu(L ¹) ₂ (H ₂ O) ₂]	3377(b)	1713(m)	1645(m)	1271(m)	-	541(m) 619(m)	1.98	1513	-	-	-	42.80
[Cu(L ²) ₂ (H ₂ O) ₂]	3363(b)	1716(m)	1631(m)	1252(m)	1568(m)	536(m) 598(w)	1.88	1493	-	-	-	42.38

Table 3 : Kinetic data of Mn(II), Fe(III), Co(II), Ni(II) and Cu(II) complexes of HL², evaluated by the Coats-Redfern method.

Complex	Step	n	E* KJ mole ⁻¹	Z S ⁻¹	ΔS* JK ⁻¹ mole ⁻¹	ΔG* KJ mole ⁻¹
[C ₃₀ H ₂₄ N ₂ O ₁₄ Mn]	1	0.7	58.63	1.185x10 ⁵	-151.9	67.51
	2	1.18	79.52	1.541x10 ⁵	-145.1	90.67
	3	0.38	14.62	2.74x10 ¹²	-84.24	22.62
[C ₃₀ H ₂₂ N ₂ O ₁₃ ClFe]	1	1.15	85.76	1.11x10 ⁸	-94.56	91.03
	2	1.62	44.75	1.66x10 ³	-188.28	57.05
	3	1.52	16.23	2.97	-244.35	40.42
[C ₃₀ H ₂₄ N ₂ O ₁₄ Co]	1	0.4	11.45	9.51x10 ⁹	-56.98	14.41
	2	0.5	10.29	1.7x10 ¹⁰	-52.86	13.28
	3	Rapid decomposition could not be studied				
	4	0.64	13.71	7.21x10 ⁸	-83.81	22.02
[C ₃₀ H ₂₄ N ₂ O ₁₄ Ni]	1	0.91	42.71	2.62x10 ³	-182.3	51.99
	2	0.92	24.94	10.89	-229.9	39.67
	3	0.91	8.426	0.052	-278.3	37.65
[C ₃₀ H ₂₄ N ₂ O ₁₄ Cu]	1	0.93	30.22	40.62	-217.2	41.48
	2	1.1	56.97	8.26x10 ³	-175.4	69.04
	3	0.95	15.23	4.388	-241.6	40.59

Table 4: Comparison of the X-ray powder diffraction data of MnO, FeO, CoO, NiO and CuO.

Metallic Residue	System	Lattice constants	Observed		Reference		
			Angle 2θ	d-value(Å)	Angle 2θ	d-value(Å)	JCPDS-ICDD number
MnO	cubic	a = b = c = 4.442	34.960	2.5644	34.958	2.5645	78-0424
			40.574	2.2216	40.587	2.2210	
			58.740	1.5706	58.745	1.5704	
			71.234	1.3227	70.220	1.3393	
			73.845	1.2822	73.843	1.2822	
FeO	cubic	a = b = c = 4.294	36.198	2.4796	36.204	2.4791	75-1550
			42.072	2.1460	42.051	2.1470	
			60.982	1.5181	60.980	1.5181	
			73.024	1.2946	73.021	1.2946	
			76.842	1.2326	76.841	1.2395	
CoO	cubic	a = b = c = 4.262	36.487	2.4604	36.486	2.4606	75-0533
			42.405	2.1298	42.381	2.1310	
			61.492	1.5067	61.488	1.5068	
			73.658	1.2850	73.659	1.2850	
			77.532	1.2302	77.525	1.2303	
NiO	cubic	a = b = c = 4.176	37.255	2.4116	37.263	2.4111	75-0269
			43.274	2.0891	43.296	2.0881	
			62.850	1.4771	62.893	1.4765	
			75.419	1.2594	75.433	1.2591	
			79.409	1.2058	79.427	1.2055	
CuO	cubic	a = b = c = 4.245	36.630	2.4512	36.637	2.4508	78-0428
			42.614	2.1198	42.559	2.1225	
			61.766	1.5007	61.761	1.5008	
			74.008	1.2798	74.00	1.2799	
			77.877	1.2256	77.893	1.2254	

REFERENCES

- [1] D.Kumar, S.P. Singh, J.Indian Chem.Soc. 83 (2006) 419.
- [2] M. Gobor, S. Janos, T. Szell, G. Sipo, Acta.Microbiol. Acad. Sci. 1 (1967) 45.
- [3] C. O. Adewunmi, F. O. Ogungbamila, J. O. Oluwadiya, Planta Medica 53 (1987) 110.
- [4] G. S. B. Viana, M. A. M. Bandeira, F. J. A. Matos, *Allemão Phytomedicine* 10(2-3) (2003) 189.
- [5] E. C. Torres-Santos, D. L. Moreira, M. A. C. Kaplan, M. N. Meirettes, B. Rossi-Bergmann, *Antimicrobial Agents Chemother* 43 (1999) 1234.
- [6] L. Miranda, J. F. Cristobal, Stevens, Vadim Ivanov, Mack McCall, Balz Feri, M. L. Deinzer, D. R. Buhler, *J. Agric. Food. Chemistry* 48(9) (2000) 3876.
- [7] D. Azarifar, H. Ghasemnejad, *Molecules* 8 (2003) 642.
- [8] A. O. Oyedapo, V. O. Makanju, C.O.Adewunmi, E.O.Iwalewa and .K.Adenowo., *Afr. J. Trad. CAM.* 1 (2004) 55.
- [9] V.D. John, G. Kuttan, K. Krishanankutty, *J.Exp.Clin.Can.Res.* 33 (2002) 343.
- [10] K.K. Soudamani, R. Kuttan, *Ethnopharmacol* 27 (1989) 227.
- [11] T.S. Rao, N. Basu, H.H. Siddique, *Ind.J.Med.Res.* 75 (1982) 574.
- [12] J.D.Lasken, A.H. Conney, *Carcinogenesis* 13 (1992) 2183.

- [13]R.J. Anto, K.N. Dinesh Babu, R. Kuttan, *Cancer.Lett.*94 (1995) 74.
- [14]V. N. Patange, B. R. Arbad, V. G. Mane, S. D. Salunke, *Trans. Met. Chem.* 32 (2007) 944.
- [15]V. N. Patange, B. R. Arbad, *Indian. J. Chem. Soc.* in the press Vol 84 Nov 2007
- [16]V.G.Mane, V. N. Patange, B. R. Arbad, *Indian. J. Chem. Soc.* in the press Vol 84 Nov 2007.
- [17]N. Ramarao, V.P. Rao, V.J. Tyaga Raju, M.C. Ganorkar, *Indian.J.Chem.* 24(A) (1985) 877.
- [18]O. Carugo, C.B. Castellani, M. Rizzi, *Polyhedron* 9 (1990) 2061.
- [19]K. Nakamoto, *Infrared Spectra Of Inorganic And Coordination Compounds*, Wiley Interscience, New York, (1970), pp 159, 167, 214.
- [20]P. Venketeswar Rao, A. Venkata Narasaiah, *Indian.J.Chem.* 42(A) (2003) 896.
- [21]G.L. Eichhorn, J.C. Bailar, *J. Am.Chem.Soc.*75 (1953) 2905.
- [22]B.N. Figgis, *Introduction to ligand fields*, Interscience, London, 1966 ,p.218.
- [23]L.Sacconi, *Trans.Met.Chem.* 61 (1968) 943.
- [24]A.B.P. Lever, *Inorganic electronic spectroscopy* (Elsevier Amsterdam), 1968, p.275-361.
- [25]K.C. Satpatty, A.K. Panda, R. Mishra, I. Pande, *Trans.Met.Chem.*16 (1991) 410.
- [26]M.N. Patel, V.J. Patel, *Synth.React.Inorg.Met.Org.Chem.*19 (1989) 137.
- [27]A. W. Coats, J. P. Redfern, *Nature* 201 (1964) 68.
- [28]G.G. Mohamed, C.M.Sharaby, *Spectrochim Acta A* 66(4-5) (2007) 949.
- [29]J.R. Carvajal, T. Roisnel, Winplotr, a graphic tool for powder diffraction, Laboratoire Leon Brillouin (cea/enrs) 91191 gif suryvette cedex, France, 2004.
- [30]D.P. Shoemaker, C.W. Garland, *Experiments in physical chemistry*, 5th ed., McGraw-Hill international editions, New York, 1989, p.17-27
- [31]B.D. Cullity, *Elements of X-rays Diffraction*, Addison-Wesley, Massachusetts, 1965, p.261.
- [32]H.H. Thornberry, *Phytopathology* 40 (1950) 419.
- [33]B.S.Bhist, R.D.Khulbe, *Indian.Phyto.Pathology* 40(4) (1995) 480.